Journal of the Physical Society of Japan
Vol. 71, No. 5, May, 2002, pp. 1226–1229
©2002 The Physical Society of Japan

Charge and Spin Order in $RNiO_3$ (R=Nd, Y) by LSDA+U Method

Susumu YAMAMOTO and Takeo FUJIWARA

Department of Applied Physics, University of Tokyo, 7-3-1 Hongo, Bunkyo-ku, Tokyo 113-8656

(Received November 12, 2001)

Electronic structures of $NdNiO_3$ and $YNiO_3$ are calculated by using the LSDA+U method with rotational invariance. No orbital order on Ni sites is observed in the calculations for the two systems. Different types of charge ordering are found in the two systems. In a small distorted system $NdNiO_3$, all nickel ions are trivalent, while oxygen sites show charge ordering and spin density polarization in the energy range of Ni e_g σ^* band. In a large distorted system $YNiO_3$, charge disproportionation occurs. Therefore, the charge ordering stabilizes the asymmetry of the arrangement of Ni magnetic moments in both systems.

KEYWORDS: perovskite nickelates, charge order, spin order, LSDA+U
DOI: 10.1143/JPSJ.71.1226

Perovskite transition metal oxides are currently of high interest because of the large variety and the possible controllability of their physical properties. Perovskite nickelates $RNiO_3$ (R = a trivalent rare earth or Y ion) can be classified into three different categories, according to their tolerance factor ($t = d_{R-O}/\sqrt{2}d_{Ni-O}$).[1–5] One category is for compounds whose tolerance factor is very small ($t < 0.91$) and that have a large distortion, such as $LuNiO_3$ or $YNiO_3$. They are antiferromagnetic insulators at low temperatures. This class of $RNiO_3$ undergoes transition to a paramagnetic insulator at the Neel temperature T_N and also has another phase transition from paramagnetic insulator to paramagnetic metal (M–I transition) at very high transition temperature. Second is those whose tolerance factor is intermediate ($0.91 < t < 0.93$), such as $NdNiO_3$ or $PrNiO_3$. These materials are also antiferromagnetic insulators at low temperatures and above T_N they are paramagnetic metals.[6] Third is $LaNiO_3$ where $t = 0.94$; it is a paramagnetic metal.

The low-temperature phase of above-mentioned first and second classes of $RNiO_3$ exhibits unique magnetic structures.[1–4] Its magnetic diffraction peak is characterized by the propagation vector $\boldsymbol{k} = (1/2, 0, 1/2)$ and the magnetic unit cell is identified as the $2 \times 1 \times 2$ supercell of the crystallographic lattice.[1,4] The magnetic order is specified to be alternating ferromagnetic (FM) and antiferromagnetic (AFM) couplings $\cdots Ni^{\uparrow} -\overset{FM}{O}- Ni^{\uparrow} -\overset{AFM}{O}- Ni^{\downarrow} -\overset{FM}{O}- Ni^{\downarrow} -\overset{AFM}{O}- Ni^{\uparrow} -\overset{FM}{O}- Ni^{\uparrow} \cdots$ along three crystallographic directions.

Contrary to the asymmetric arrangement of magnetic bonds (FM/AFM) around each nickel site, Ni–O distances around each Ni ion are almost equal. For instance, the difference between the longest and the shortest Ni–O bonds in one NiO_6 octahedron is at most 2% in $RNiO_3$.[1,3,5] The Jahn–Teller distortion is absent in $RNiO_3$, even in the largely distorted system $YNiO_3$, whose tolerance factor is 0.88. Experimentally, there is only one crystallographic site for Ni ions in $NdNiO_3$ and two different sites for Ni ions in $YNiO_3$. Therefore, one can expect trivalent ions Ni^{3+} in $NdNiO_3$. In contrast, Ni ions in $YNiO_3$ are divalent and quadrivalent, i.e., the charge disproportionation $2Ni^{3+} \rightarrow Ni^{2+} + Ni^{4+}$ occurs.

In this letter, we study the electronic properties of the AFM insulating phase of two perovskite nickelates, $NdNiO_3$ and $YNiO_3$, which are typical of the above-mentioned two respective classes. We use the LSDA+U method with rotational invariance in conjunction with the LMTO-ASA method.[7] The Hamiltonian of the LSDA+U method includes the Hartree–Fock-type term for the electron-electron interaction between localized orbitals. The ionic positions and lattice parameters used in the present calculations are imported from the diffraction experiments.[1,4] The unit cell here is the $2 \times 1 \times 2$ crystallographic supercell containing 16 Nd or Y ions, 16 Ni ions, 48 O ions, and 32 empty spheres, thus a total of 112 atomic spheres. Sixty-four k-points in the Brillouin zone are sampled in the calculation of the density of states. $NdNiO_3$ is antiferromagnetic up to $T_N = 200\,K$, but the Nd spin moment vanishes at about 30 K.[2] Therefore, the three 4f electrons of Nd ion do not play an essential role in the spin ordering of Ni ions and are counted in the frozen core. We also calculated the electronic structure of $NdNiO_3$ with 4f electrons in valence states, and the resultant structure of Ni d e_g bands shows no significant difference. The Coulomb and exchange parameters U and J of Ni ions are fixed to be 7.0 eV and 0.88 eV, respectively, for all the LSDA+U calculations. These values are consistent with photoemission experiments and the results of the LSDA calculations.[8,9] Calculated results do not change significantly over a large range of values for U and J.

The crystallographic space groups of $NdNiO_3$ and $YNiO_3$ are orthorhombic *Pbnm* and monoclinic $P2_1/n$, respectively. The group theoretical analysis shows that, using the projection operator method, the Jahn–Teller distortion of one NiO_6 octahedron cannot be transferred over the entire enlarged $2 \times 1 \times 2$ supercell with $\boldsymbol{k} = (1/2, 0, 1/2)$.[10] Therefore, the Jahn–Teller distortion cannot actually appear in the observed spin-ordered state.

$NdNiO_3$: There are two possible spin configurations in $NdNiO_3$ satisfying the observed transfer vectors $\boldsymbol{k} = (1/2, 0, 1/2)$. One is that the spin magnetic moments align ferromagnetically on the (101) plane and the planes are stacked with a doubled period as $\uparrow\uparrow\downarrow\downarrow\uparrow\uparrow\downarrow\downarrow \cdots\cdots$, whose magnetic space group is monoclinic P_ba.[11] This spin configuration is assumed in the present letter. Another possible spin configuration with $\uparrow\uparrow\downarrow\downarrow$ spin order is the doubled period checkerboard stacking along crystallographic y-axis, in which case the magnetic space group is

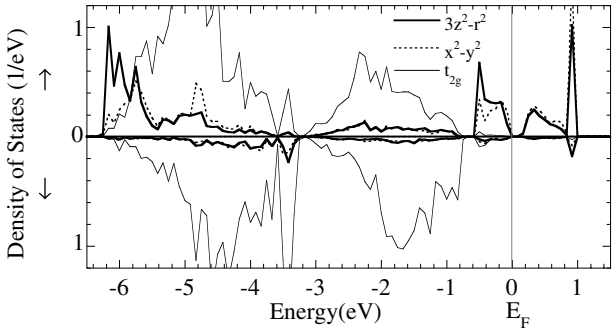

Fig. 1. Projected density of states of trivalent nickel Ni^{3+} in $NdNiO_3$. The zero energy is set at the top of the occupied states E_F. The local z-axis directs from Ni to one of the oxygen atoms with the longest Ni–O distance, and the local x- and y- axes to the appropriate O atoms.

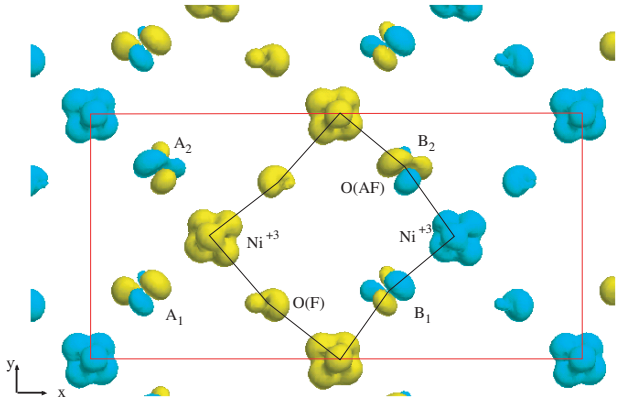

Fig. 2. Isometric surface of the spin density $\rho_\uparrow - \rho_\downarrow = \pm 0.01$ states/(atomic unit)^3 in the energy range $E_F - 0.6\,eV \sim E_F$ in a thin slab parallel to the (001) plane. Yellow and blue surfaces indicate the plus and minus spin densities, respectively. Black solid lines represent Ni–O bonds and red lines represent unit cell. The position of oxygen atom A_1 is equivalent to that of A_2 in crystallographic space group *Pbnm*, while no operation can transfer A_1 to A_2 in the magnetic space group P_ba. The position A_i ($i = 1, 2$) is equivalent to the position B_i with translation in *Pbnm*, and in the magnetic space group P_ba, this operation is accompanied by the time-reversal operator.

orthorhombic C_amc2_1.[11] The state of C_amc2_1 shows orbital ordering of e_g states on Ni sites, but the resultant total energy in the present calculation is higher by 0.18 eV per $2 \times 1 \times 2$ cell than that of P_ba. Because there is no possibility of subsidiary Jahn–Teller distortion to lower the total energy, C_amc2_1 may not be the symmetry to be considered. The total energy is also calculated in a fictitious antiferromagnetic state of $Pb'nm'$ whose magnetic unit cell is identical to the crystallographic one and is higher by 2.0 eV per $1 \times 1 \times 1$ cell.

Figure 1 shows the projected density of states on the Ni 3d orbitals in $NdNiO_3$. The system is an insulator with a gap $E_g = 0.11$ eV. Each nickel ion has the local magnetic moment $\pm 1.1\,\mu_B$ within the atomic sphere of a radius 2.51 au, in contrast to the observed value of $\pm 0.9\,\mu_B$.[2] It should be noted that the local magnetic moment cannot be uniquely defined. Furthermore, $NdNiO_3$ is not a simple antiferromagnetic insulator but a dynamical effect is essential, which may be the reason for this discrepancy.[6] There is no distinctive variation in partial spin density of states of Ni site in each magnetic sublattice. An e_g band lies in the energy range $E_F - 0.6\,eV \sim E_F + 1.2\,eV$. The states in the energy range $E_F - 0.6\,eV \sim E_F$ consist of occupied e_g states, one state per Ni ion and totally 16, and those in the energy range $E_F + 0.1\,eV \sim E_F + 1.2\,eV$ consist of vacant e_g states, one per Ni ion and totally 16. In fact, these e_g orbitals extend over surrounding oxygen sites from Ni ions due to strong hybridization between Ni e_g and O p orbitals. The extended occupied e_g orbital has 60% weight on p orbitals of the surrounding six oxygens, and 10% weight on one individual oxygen. Therefore, one would establish a model where one occupied e_g state with majority spin locates at the top of the valence bands, and it hybridizes strongly with the p states on nearby O ions. This is the molecular orbital σ^* state.[12] Then one can assign all nickel ions in $NdNiO_3$ to be trivalent Ni^{3+} ($t_{2g}^6 e_g^1$), even though the Ni ion is not truly ionized by +3 charge. In the projected density of states of the Ni ion site, one observes a large number of e_g states at the bottom of the d bands, which are the bonding states between Ni d and O p, corresponding to the σ states in the molecular orbital picture.[12]

The e_g band in the range $E_F - 0.6\,eV \sim E_F$ does not show any orbital ordering. In fact, off-diagonal elements within the e_g subblock of the occupation matrix $\{n_{mm'}\}$ are zero and the diagonal elements are identical. The [111] axis of the perovskite cubic lattice would be perpendicular to the (101) plane of the present lattice (P_ba structure). This [111] axis of the cubic lattice corresponds to the [201] axis of the present lattice. The absence of the orbital ordering is due to the fact that the [201] axis of the present lattice has threefold rotational symmetry in the ideal cubic lattice.[13] Due to this pseudo threefold rotational symmetry, the basis orbitals of E_g representation of the trigonal group D_{3d} is a good basis set and those derived from e_g orbitals are $\varphi_{u+} = -\frac{1}{\sqrt{2}}(\varphi_{3z^2-r^2} + i\varphi_{x^2-y^2})$ and $\varphi_{u-} = \frac{1}{\sqrt{2}}(\varphi_{3z^2-r^2} - i\varphi_{x^2-y^2})$. Therefore, there is no difference between the occupancies of $\varphi_{3z^2-r^2}$ and $\varphi_{x^2-y^2}$.

Figure 2 is the spatial profile of spin densities $\rho_\uparrow - \rho_\downarrow$ in the energy range $E_F - 0.6\,eV \sim E_F$ (σ^* state). Only one spin component of O p orbitals on the FM bond bridges the two Ni e_g orbitals, while both spin components on the AFM bond couple with Ni e_g orbitals of respective spins. Consequently, oxygen ions on the AFM bond have more charge in this energy range than oxygen on the FM bond. This is the realization of the oxygen-site charge-ordered state which was discussed by Mizokawa *et al.* in the framework of the Hartree–Fock calculation.[14] However, the charge difference between oxygen sites of $Ni^{\uparrow} - \overset{FM}{O} - Ni^{\uparrow}$ and $Ni^{\uparrow} - \overset{AFM}{O} - Ni^{\downarrow}$ in σ^* states is mostly compensated by hybridized σ state at low energies. Moreover, no oxygen ion has local magnetic moment.

The magnetic space group is P_ba and its unitary part is Pa. The unit cell and lattice primitive vectors are not identical to those in the crystallographic space group *Pbnm*. The former has orthorhombic symmetry while the latter has monoclinic symmetry. One glide reflection in *Pbnm* transfers the atomic site A_1 to A_2 in Fig. 2. However this operation or that accompanied by the time-reversal operator is not an element in the magnetic space group P_ba. Therefore, the spin-density polarizations around A_1 and A_2 are inequivalent. The symmetry lowering of the unitary part Pa, associated with U, is the origin of the opening of the band gap at E_F in the

majority spin band, despite the absence of the orbital ordering on Ni sites (i.e., symmetry driven band gap). Therefore, one can conclude that the origin of the insulating phase at low temperatures in $NdNiO_3$ is the characteristic spin density on the oxygen sites. In fictitious ideal cubic structure without distortion or tilting of NiO_6 octahedra, the system becomes metal wherein valence and conduction bands touch at a few isolated k-points with each other.[10] The choice of the value of U does not affect the structure of σ^* bands. The value of the band gap is unchanged down to $U = 4\,\mathrm{eV}$. This is because the gap is driven by symmetry under the finite U.

$YNiO_3$: One should expect large distortion in $YNiO_3$ because $YNiO_3$ is the typical system with the small tolerance factor.[4,5] There are two different crystallographic Ni sites, and the distances from each Ni ion to surrounding O ion are different by 3–4% from one type of Ni ion to another.[4] The calculated self-consistent solution is that with the apparent charge disproportionation and no orbital polarization. Since the Ni^{4+} site has no spin magnetic moment, the two spin configurations discussed in $NdNiO_3$ become identical and the spin configuration of $YNiO_3$ is uniquely determined. The magnetic space group is P_b2_1 if the spins of Ni^{4+} ions are nonvanishing and, P_b2_1/a if the spins of Ni^{4+} ions are zero. The latter symmetry P_b2_1/a is actually the case.

Figure 3 shows the projected density of states at Ni ion sites. The system is an insulator with a gap $E_g = 1.03\,\mathrm{eV}$. The resultant magnetic moments for half of the Ni ions are $\pm 1.5\,\mu_B$ within the atomic sphere of a radius 2.52 au, namely divalent ions Ni^{2+} ($t_{2g}^6e_g^2$), of large NiO_6 octahedron and zero for the other half of the Ni ions within the atomic sphere of a radius 2.51 au, namely quadrivalent Ni^{4+} (t_{2g}^6), of small octahedron. The experimentally observed magnetic moments are $\pm 1.4\,\mu_B$ for Ni^{2+} ions and $\pm 0.7\,\mu_B$ for Ni^{4+} ions.[4] The discrepancy may be due to a possible non-collinear spin order. The number of states in the energy range $E_F - 0.47\,\mathrm{eV} \sim E_F$ is 16 with dominant weight on Ni^{2+}. Because the number of Ni^{2+} in the $2 \times 1 \times 2$ cell is 8, these states are determined to be two e_g states mainly on Ni^{2+} and surrounding oxygens. The σ^* bands of Ni^{4+} e_g orbitals are shifted to the higher energy region ($>E_F + 1\,\mathrm{eV}$) without spin polarization.

A large number of Ni e_g orbitals (σ bands of Ni e_g and O p orbitals) locate at the bottom of the d bands, in the range $E_F - 6.7\,\mathrm{eV} \sim E_F - 5.8\,\mathrm{eV}$ for Ni^{2+}, and in the range $E_F - 5\,\mathrm{eV} \sim E_F - 4\,\mathrm{eV}$ for Ni^{4+}. Almost one electron per nickel ion (Ni^2+ or Ni^4+) participates in the respective σ band. From these facts, one can establish a model wherein deep σ molecular orbitals stabilize the system, and the other two e_g states (σ^* states) per Ni^{2+} ion located at $E_F - 0.47\,\mathrm{eV} \sim E_F$.

The charge disproportionation is mainly due to the crystal field effect. The low spin state in Ni^{4+} or Ni^{3+} ion is energetically unstable in the small Dq case and the ground state multiplet of Ni^{2+} is $^3A_2$ ($t_{2g}^6e_g^2$) for all arbitrary values of Dq.[15] Therefore, the small tolerance factor causes two different Ni sites, compressed Ni^{4+} (large Dq) and dilated Ni^{2+} (small Dq), rather than uniformly dilated Ni^{3+} ionic states.[16] The standard value of Dq/B (B is the Racah parameter) for Ni^{2+} is presumably around 1.0. Once one estimates the crystal field effects from the Ni–O bond lengths d_{Ni-O}, the difference of $10Dq$ on two Ni ion sites is presumably about 20%.

Two narrow e_g bands can be seen in the energy ranges $E_F - 0.47\,\mathrm{eV} \sim E_F - 0.23\,\mathrm{eV}$ and $E_F - 0.23\,\mathrm{eV} \sim E_F$ in Fig. 3(a). Two Ni^{2+} e_g states are spatially extending over a wide area and not only hybridizing with the nearest neighbor O ions but also extending over the nearest Ni^{4+} ions. This situation is well depicted in the spin density. Figure 4 shows the isometric surfaces of the spin density in the range of $E_F - 0.47\,\mathrm{eV} \sim E_F - 0.23\,\mathrm{eV}$. The d-wave-functions on Ni^{2+} (σ^* states) are extending along the direction of the neighboring Ni^{4+}, and antiferromagnetically coupled with other Ni^{2+} ions. The charge in each Ni ion is compensated in $YNiO_3$ as in $NdNiO_3$ and the difference

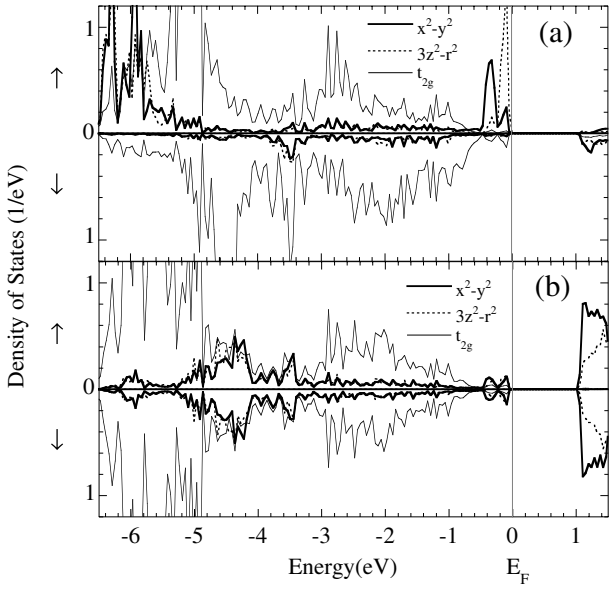

Fig. 3. Projected density of states of (a) divalent Ni^{2+} and (b) quadrivalent Ni^{4+} in $YNiO_3$. The zero energy is set at the top of the occupied states E_F. The local coordinate axes are chosen in the same manner for those in Fig. 1.

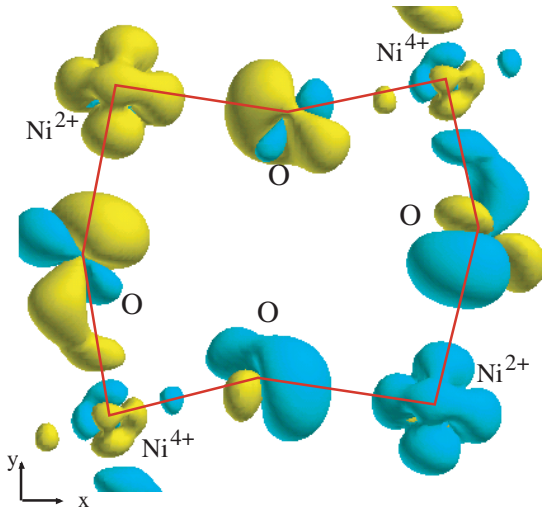

Fig. 4. Isometric surface of spin density $\rho_\uparrow - \rho_\downarrow = \pm 0.002$ states/(atomic unit)^3 in the energy range of an e_g band ($E_F - 0.47\,\mathrm{eV} \sim E_F - 0.23\,\mathrm{eV}$) in a thin slab parallel to the (001) plane. Yellow surface means the sign of the spin density is plus, blue one means minus.

between total charges in the muffin tin spheres on Ni^{2+} and Ni^{4+} sites is very small, equals to 0.03. This variation is the same order as that of oxygen ions in $NdNiO_3$. However, charge disproportionation is coupled with the lattice distortion, where large oxygen octahedron is surrounding Ni^{2+}, and stabilizes the lattice system in $YNiO_3$. Therefore, a diffraction experiment can detect the charge ordering in the yttrium system easier than in the neodymium system.

In conclusion, we have studied two typical antiferromagnetic insulating phases of $RNiO_3$, $NdNiO_3$ and $YNiO_3$, by using the LSDA+U method. The possibility of the Jahn–Teller distortion is excluded by the group theoretical consideration in ref. 10. No orbital order on Ni sites is observed in either of the two systems, but two different types of ordering are observed. In small-distortion $RNiO_3$ such as $NdNiO_3$, oxygen sites show the charge ordering and spin density polarization, and this is the origin of the gap opening in $NdNiO_3$. In large-distortion $RNiO_3$ such as $YNiO_3$, charge disproportionation $2Ni^{3+} \rightarrow Ni^{2+} + Ni^{4+}$ occurs. The charge ordering mechanism can explain the stabilization of the asymmetric alignment of the local magnetic moments around each nickel site in both systems.

We add a final comment on the effects of electron-electron correlation in $RNiO_3$. The widths of the calculated e_g bands D by the LDA are 2.82 eV ($YNiO_3$), 2.87 eV ($NdNiO_3$), and 3.18 eV ($LaNiO_3$). Therefore, the ratio of U/D can be estimated to be $1 : 0.98 : 0.89$, assuming the value of the Coulomb repulsion U is common for all. One can see a large reduction of U/D in $LaNiO_3$, which may be the key parameter for the difference of the ground states of these perovskite nickelates. $NdNiO_3$ shows the anomalous M–I transition.[6] $LaNiO_3$ is presumably an anomalous metal of strongly correlated electrons[17] and could not be treated within the framework of the LSDA+U method.

The authors are very grateful to V. I. Anisimov for helpful advice on the LSDA+U method and for a fruitful discussion on the spin alignment of $NdNiO_3$, and also to T. Mizokawa for useful discussion about their work.[14] This work is supported by Grant-in-Aid for COE Research ''Spin-Charge-Photon''.

1) J. L. García-Muñoz, J. Rodríguez-Carvajal, P. Lacorre and J. B. Torrance: Phys. Rev. B **46** (1992) 4414.
2) J. L. García-Muñoz, J. Rodríguez-Carvajal and P. Lacorre: Phys. Rev. B **50** (1994) 978.
3) J. Rodríguez-Carvajal, S. Rosenkranz, M. Medarde, P. Lacorre, M. T. Fernandez-Díaz, F. Fauth and V. Trounov: Phys. Rev. B **57** (1998) 456.
4) J. A. Alonso, J. L. García-Muñoz, M. T. Fernandez-Díaz, M. A. G. Aranda, M. J. Martínez-Lope and M. T. Casais: Phys. Rev. Lett. **82** (1999) 3871.
5) J. A. Alonso, M. J. Martínez-Lope, M. T. Casais, J. L. García-Muñoz and M. T. Fernandez-Díaz: Phys. Rev. B **61** (2000) 1756.
6) T. Katsufuji, Y. Okimoto, T. Arima, Y. Tokura and J. B. Torrance: Phys. Rev. B **51** (1995) 4830.
7) A. I. Liechtenstein, V. I. Anisimov and J. Zaanen: Phys. Rev. B **52** (1995) R5467.
8) A. E. Bocquet, T. Mizokawa, T. Saitoh, H. Namatame and A. Fujimori: Phys. Rev. B **46** (1992) 3771.
9) V. I. Anisimov, J. Zaanen and O. K. Andersen: Phys. Rev. B **44** (1991) 943.
10) S. Yamamoto and T. Fujiwara: to be published in *Proc. 8th ISSP Int. Symp. Correlated Electrons, Kashiwa, 2001* (Elsevier, 2002).
11) S. C. Miller and W. F. Love: *Tables of Irreducible Representations of Space Groups and Co-Representations of Magnetic Space Group* (Pruett Press, Boulder, Colorado, 1967).
12) S. Sugano and R. G. Shulman: Phys. Rev. **130** (1963) 517.
13) The unit cell of the crystallographic *Pbnm* structure can be obtained from the simple cubic perovskite structure as follows; (i) rotate by $\frac{\pi}{4}$ around the [001] axis, (ii) make the $\sqrt{2} \times \sqrt{2} \times 2$ supercell with the distortions. The [110] axis of the cubic lattice is parallel to the x-axis of the *Pbnm* structure. The unit cell of the P_ba structure corresponds to the $2\sqrt{2} \times \sqrt{2} \times 4$ supercell of the cubic cell, as in Fig. 2.
14) T. Mizokawa, D. I. Khomskii and G. A. Sawatzky: Phys. Rev. B **61** (2000) 11263.
15) S. Sugano, Y. Tanabe and H. Kamimura: *Multiplets of Transition-metal Ions in Crystals* (Academic Press, New York, 1970).
16) The value of $10Dq$, the parameter of the crystal field, is proportional to $d_{\mathrm{Ni-O}}^{-5}$.
17) J.-S. Zhou, J. B. Goodenough, B. Dabrowski, P. W. Klamut and Z. Bukowski: Phys. Rev. Lett. **84** (2000) 526.